

PAPER • OPEN ACCESS

Quantifying the Predictability of a ‘Dunkelflaute’ Event by Utilizing a Mesoscale Model


To cite this article: Bowen Li *et al* 2020 *J. Phys.: Conf. Ser.* **1618** 062042

View the [article online](#) for updates and enhancements.

You may also like

- [Isolation, Purification and Characterization of \$\alpha\$ -Lactalbumin from Camel Milk and Study its Antioxidant Activity in Oils](#)
Zaid A. Haddad and Kifah Saed Doosh
- [Effectiveness of the renovation in Moscow based on calculations of static and dynamic indicators](#)
Svetlana Kolobova
- [Optimal Prediction of Atmospheric Turbulence by Means of the Weather Research and Forecasting Model](#)
Alohotsy Rafalimanana, Christophe Giordano, Aziz Ziad *et al.*





The
Electrochemical
Society

Advancing solid state &
electrochemical science & technology

DISCOVER
how sustainability
intersects with
electrochemistry & solid
state science research

Quantifying the Predictability of a ‘Dunkelflaute’ Event by Utilizing a Mesoscale Model

Bowen Li¹, Sukanta Basu¹, Simon J. Watson², Herman W. J. Russchenberg¹.

¹Faculty of Civil Engineering and Geosciences, Delft University of Technology, Delft, The Netherlands.

²Faculty of Aerospace Engineering, Delft University of Technology, Delft, The Netherlands.

E-mail: B.Li-1@tudelft.nl

Abstract. In the coming decades, both wind and solar power production will be playing increasingly important roles in Europe’s energy economy. It is absolutely essential that power grids are resilient against any unusual weather phenomena. One such meteorological phenomenon, “Dunkelflaute”, is causing serious concern to the renewable energy industry, which is primarily characterized by calm winds and overcast conditions. For example, a Dunkelflaute event happened in the Netherlands on 30th April 2018 leading to a significant shortfall in renewable energy generation requiring emergency intervention by the system operator. By analyzing this case, this paper investigates the performance of a state-of-the-art mesoscale model, Weather Research and Forecasting (WRF), in forecasting a Dunkelflaute event. Multiple WRF simulations are driven using real-time Global Forecast System (GFS) operational data over a range of prediction horizons. For comparison, a benchmark run is carried out using ERA5 reanalysis data as boundary conditions. Through validation using a variety of measured data covering onshore and offshore areas, wind speed is shown to be more predictable than cloud-cover in this particular case study.

1. Introduction

It is projected that by 2030, wind and solar energy production will cover a substantial proportion of energy demand in the Netherlands, and in Europe at large [1]. Renewables produced 6% of energy in the Netherlands in 2016; however, this is expected to double ($\sim 12.4\%$) in 2020, and to further grow to $\sim 27.6\%$ by 2035 [2]. Such high penetration of renewables in the next-generation power grids may render them more vulnerable to intrinsic variability and limited predictability of weather events. In this context, the so-called ‘Dunkelflaute’ events [3] are of serious concern for the renewable energy industry. Heavy overcast skies and weak wind conditions are associated with these meteorological events which can last from a few hours to a few consecutive days.

On 30th April 2018, an unexpected Dunkelflaute event occurred over the southern part of the North Sea and caused a large imbalance in renewable power generation and overall consumption. Given the acuteness of the situation, TenneT – the main transmission system operator for Germany and the Netherlands – had to issue an emergency alert in the Netherlands [4, 5]. The crisis could not be avoided by simple load management or by making use of reserve power; instead, substantial amount of electricity had to be imported from neighboring countries at high market price.



It is important to stress that this Dunkelflaute event was not an isolated episode. As a matter of fact, over the past few years, several Dunkelflaute events occurred in Belgium [6, 7], Germany [8, 9], and other countries. Some of them caused significant impacts on the power grids and electricity markets. There is no reason to believe that the occurrences of Dunkelflaute will subside in the future. Instead, with ever increasing penetration of renewables in the power grid, the (negative) impacts of Dunkelflaute events will likely become more and more detrimental. A brief climatology of Dunkelflaute event in the Netherlands is documented in Appendix A.

We believe that multi-day-ahead forecasts of Dunkelflaute events will be significant for planning operation and other precautionary measures to alleviate the impacts associated with such events in the future. The performance of mesoscale models to forecast a Dunkelflaute event is not known in the literature. As a first step, in this paper, the performance of the Weather Research and Forecasting (WRF) model to forecast a Dunkelflaute event is investigated over a range of prediction horizons.

The aforementioned Dunkelflaute event in 2018 over the Netherlands is taken as an example to quantify the predictability of such an event. We also investigate whether wind speed or cloud-cover is more (or less) predictable in this particular case study. Measured wind data and (downwelling) shortwave radiation data from various weather stations and radiosondes are used for simulation, validation and meteorological analysis.

2. Description of Case Study

The synoptic maps for 0 UTC and 12 UTC of April 30th are shown in the top panel of Figure 1. The persistent Scandinavian and Azores highs are clearly noticeable on the maps. A low pressure center was present over the continental Europe and rapidly moved towards the North Sea within a few hours. A warm front was present over the southern part of the North Sea; it was pushed further north by a cold front moving eastward. An occluded front (purple line) is visible at 12 UTC. The bottom panel of Figure 1 shows the heavy overcast conditions over the southern part of the North Sea region on both April 29th and 30th. Overall the synoptic and mesoscale setup of this case was rather complex and caused highly variable wind conditions.

3. Description of Observational Datasets

In this study, a diverse suite of observational data are used for the validation of the WRF model-based forecasts. The Seawatch wind lidar buoy is located at the Hollandse Kust (zuid) (HKZB) station [10, 11]. It provides wind profiles at 10 vertical levels with an averaging period of 10 minutes. A 200-m tall met-tower and various surface stations are located at the Cabauw observatory [12, 13]. We make use of 10-min averaged wind data and (downwelling) shortwave radiation data from this observatory. In addition, wind profiles from a multi-beam doppler radar (called TARA) from the Cabauw observatory are also utilized. Lastly, we use radiosonde data (available daily at 0 UTC and 12 UTC) from the Norderney and EDZE Essen stations. These datasets are archived in a public repository by the University of Wyoming [14]. The locations of all these meteorological stations are shown in the right panel of Figure 2.

4. Modelling Approach

In this study, we have performed two types of runs using the WRF model (version 3.9.1.1). In the first set of runs, the initial and boundary conditions are provided by the Global Forecast System (GFS) model [15]. A total of four hindcasts are performed with distinct initialization days; specifically, 1 day, 2 days, 3 days, and 5 days prior to the Dunkelflaute event. For example, the run WRF–GFS0429 is initialized at 0 UTC on the 29th April; whereas, the run WRF–GFS0425 is initialized 5 days in advance of the Dunkelflaute event.

In addition to the GFS-based forcing dataset, we also conduct a separate WRF simulation forced by the ERA5 reanalysis dataset [16] and use it as a benchmark (WRF–ERA5). It should

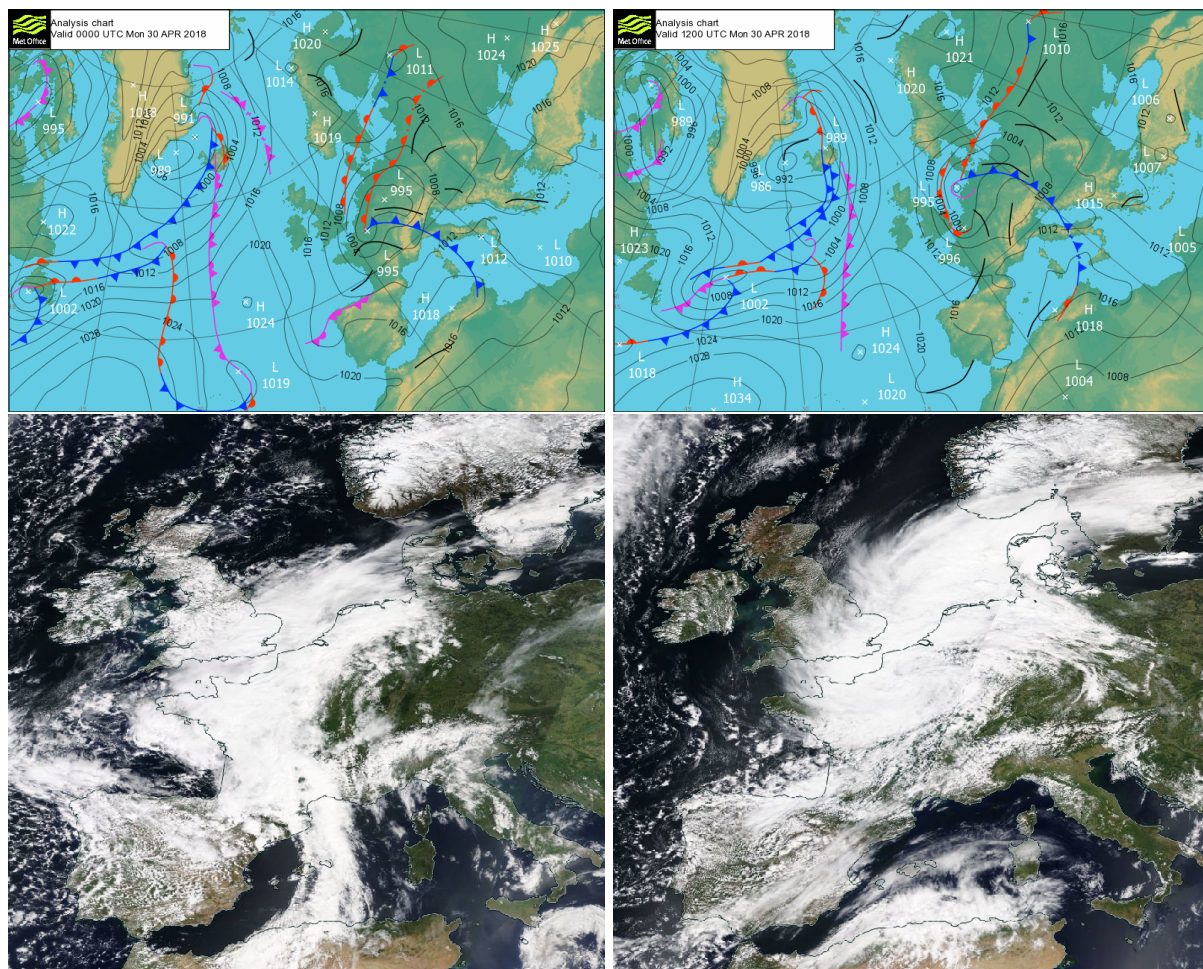


Figure 1. Synoptic analysis for 0 UTC (top-left panel) and 12 UTC (top-right panel) of 30th April, 2018. Source: <https://digital.nmla.metoffice.gov.uk/>. MODIS satellite-based reflectance maps for April 29th (bottom-left panel) and April 30th (bottom-right panel). Source: <https://worldview.earthdata.nasa.gov>.

be noted that ERA5 is a global reanalysis where a large number of observations are assimilated using a numerical weather prediction model to give the best estimate of historical meteorological parameters, whereas the GFS model produces operational forecasts whose accuracy deteriorates with increasing prediction horizon.

The GFS-based runs use a triply-nested domain with resolutions of 27 km (d01), 9 km (d02), and 3 km (d03), respectively (shown in the left panel of Figure 2). The three domains are centered over the Netherlands with time steps of 90s, 45s, and 15s, respectively. Given the higher spatial resolution of the ERA5 dataset, in this case, only two nested domains with resolutions of 9 km (d01) and 3 km (d02) are used (see the right panel of Figure 2). All the runs utilize the same physical parameterization schemes and 51 vertical levels with 14 levels in the lowest 1 km. The modeled results are output every 10 minutes for all the domains.

5. Results

In this section, we characterize the WRF model-generated hindcasts with the aid of spatial patterns, time-series, and vertical profiles. By comparing the WRF–GFS runs against the WRF–

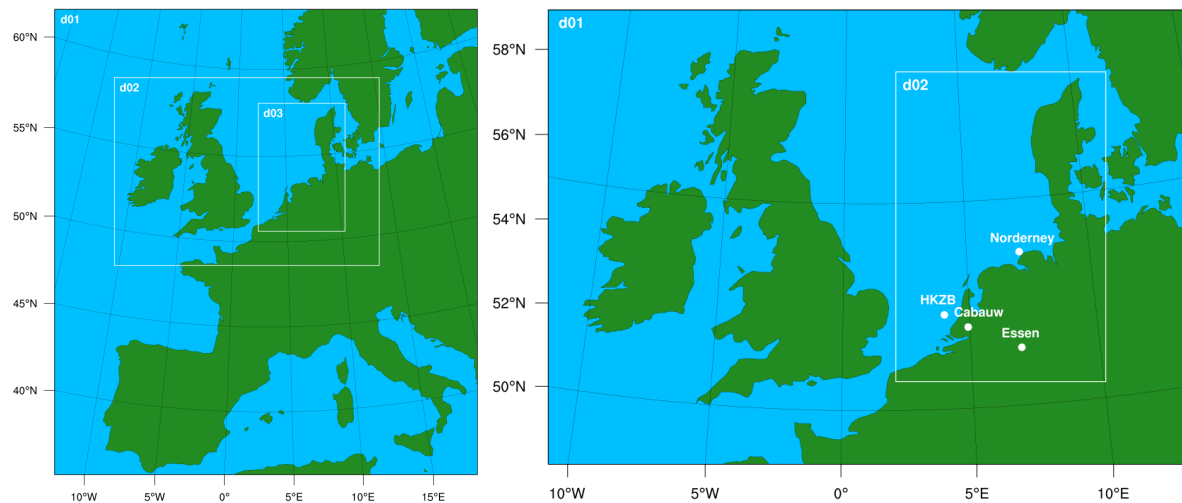


Figure 2. Domain configurations for the WRF–GFS (left panel) and the WRF–ERA5 (right panel) runs. The locations of the observation stations are overlaid on the right panel.

ERA5 run, we quantify practical predictability. In addition, by comparing the simulated results against various observational datasets, we ascertain their accuracy.

5.1. Spatial Patterns of Hub-Height Wind Speeds

In Figure 3, the simulated maps of hub-height (~ 98 m) wind speeds are depicted for 12 UTC of April 30th. According to the WRF–ERA5 simulation, extremely weak wind conditions were present at the coast of the Netherlands and Belgium. This weak flow was associated with the low pressure center. Further offshore, winds were quite strong over an extensive swath. The WRF–GFS0429, WRF–GFS0428, and WRF–GFS0425 runs more-or-less captured the overall pattern. However, some dissimilarities are discernible. For example, the weak flow region is more towards the coasts of Germany and Denmark in the case of WRF–GFS0425. Also, for this

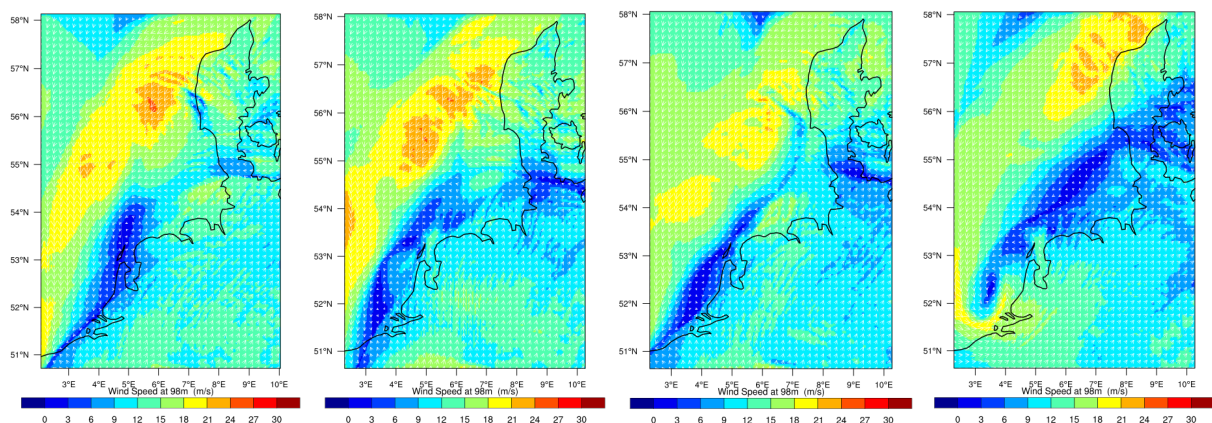


Figure 3. Simulated wind speeds at a height of approximately 98 m from the surface. From the left to right, the panels correspond to WRF–ERA5, WRF–GFS0429, WRF–GFS0428, and WRF–GFS0425 runs, respectively. Only the simulated data from the innermost domains (with grid size of 3 km) of all the WRF runs are shown in the plots. All the panels correspond to 12 UTC of April 30th, 2018.

case, strong circulations are present near the Dutch coast.

5.2. Practical Predictability

In order to quantify practical predictability, for a specific variable Φ , we compute bias (B) and root-mean-square difference (RMSD; R) as follows:

$$B(t) = \frac{1}{N_i N_j} \sum_{i=1}^{N_i} \sum_{j=1}^{N_j} [\Phi_{WRF-GFS}(i, j, t) - \Phi_{WRF-ERA5}(i, j, t)], \quad (1a)$$

$$R(t) = \sqrt{\frac{1}{N_i N_j} \sum_{i=1}^{N_i} \sum_{j=1}^{N_j} [\Phi_{WRF-GFS}(i, j, t) - \Phi_{WRF-ERA5}(i, j, t)]^2}, \quad (1b)$$

where, N_i and N_j are the grid points in the zonal and meridional directions, respectively.

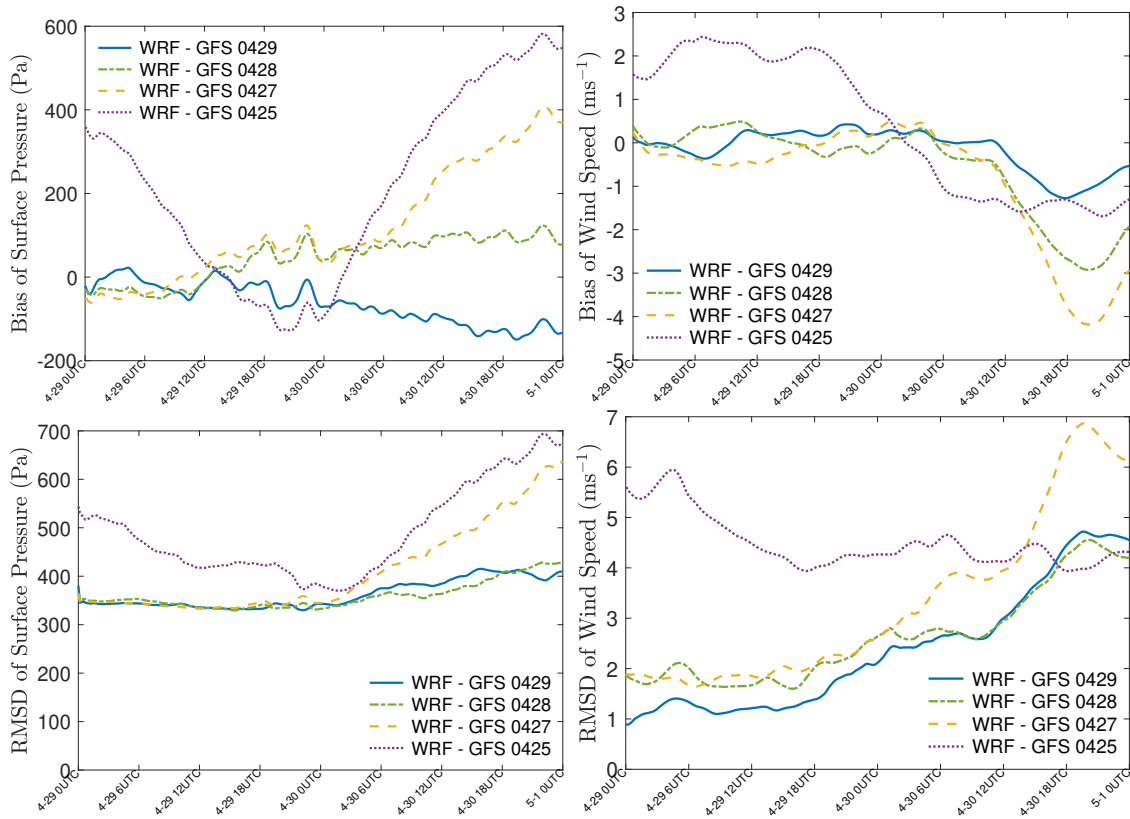


Figure 4. Time-series of bias (top panel) and RMSD (bottom panel) values from four WRF - GFS runs with respect to WRF - ERA5 run. The left and right panel correspond to surface pressure and wind speed, respectively. Only the domain-averaged data from the innermost domains (with grid size of 3 km) of all the WRF runs are shown in the plots.

In lieu of gridded observational data, we assume the WRF-ERA5-based results to be the ‘truth’. Since the modelling configurations are the same as the WRF-ERA5 run, the WRF-GFS-based results are going to deviate from this ‘truth’ because of imperfect initial and boundary conditions. Thus, it is intuitively expected that bias (B) and RMSD (R) values should increase with increasing prediction horizon. In Figure 4, we have plotted these time-series for surface

pressure (left panel) and hub-height (~ 98 m) wind speed (right panel). In these plots, each line corresponds to a specific WRF–GFS run; only the innermost domains (with grid size of 3 km) are considered.

From Figure 4, it is quite clear that the biases of all the WRF–GFS runs (with the exception of WRF–GFS0425) are close to zero for both the variables at 0 UTC of April 29th. Their magnitudes do increase with time; albeit, not in a strictly monotonic manner. The initial biases of WRF–GFS0425-based surface pressure and wind speed are rather large. They remain large with increasing time and fluctuate in erratic manners. The RMSD values (except WRF–GFS0425) are quite small at 0 UTC of April 29th. They remain small for the next 24 hours and subsequently increase with time. Based on these results, we can conclude that the surface pressure and wind conditions associated with the Dunkelflaute event of April 30th could have been reliably forecast by utilizing operational GFS data from 0 UTC of April 27th. In other words, these meteorological variables were predictable at least 3 days in advance.

5.3. Time-Series Analysis

Figure 5 shows a comparison between the WRF model-generated results and corresponding observational data from the Cabauw and HKZB stations. It is clear that there is a significant reduction in the observed wind speeds at Cabauw at around 0 UTC of April 30th. The gentle breeze lasts for more than 12 hours and hardly goes back to 10 m s^{-1} until 15 UTC of April 30th. The decrease of wind speed at HKZB occurs somewhat later on 30th April, and the wind speed is rather low for the time period 9–20 UTC. These weak wind conditions resulted in wind power generation being far below the rated output for both onshore and offshore wind farms [4].

Among all the hindcasts, the performance of the WRF–ERA5 run is the best followed by WRF–GFS0429 and WRF–GFS0428. All these runs have managed to capture the timing and magnitude of the ramp-down event of April 30th more-or-less accurately. However, the WRF–GFS0427 run has struggled to capture this drop in wind speed and the overall performance of the WRF–GFS0425 run is very poor for the entire simulation period. Based on these results from two validation locations, we can conclude that the wind speed decline seen during the Dunkelflaute event was difficult to capture by the WRF model when it was initialized longer than three days in advance by the GFS data.

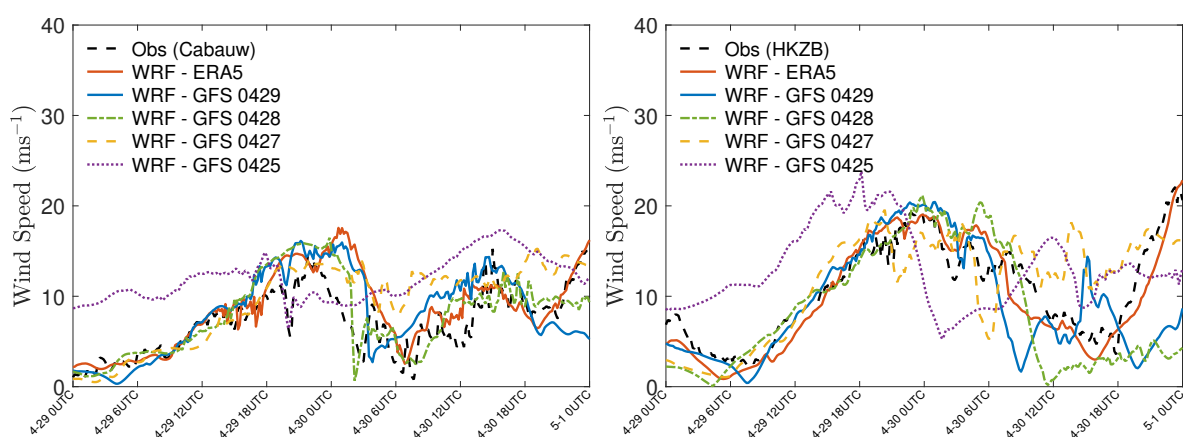


Figure 5. Observed and simulated time-series of wind speed from the Cabauw tower (left panel) and the HKZB station (right panel). Only the simulated data from the innermost domains (with grid size of 3 km) of all the WRF runs are shown in the plots.

The left and middle panels of Figure 6 display maps of simulated (downwelling) shortwave radiation at the surface from the WRF–ERA5 run. It is apparent that the simulated cloud

cover changed significantly from 12 UTC of April 29th to 12 UTC of April 30th. However, in comparison to the MODIS data (see the bottom panel of Figure 1), the cloud cover was less extensive in the simulated results. The time-series data shown in the right panel of Figure 6 corroborate this finding. All the WRF-based hindcasts reproduced the (downwelling) shortwave radiation values at the Cabauw location on April 29th; however, they substantially overestimate the (downwelling) shortwave radiation values on April 30th.

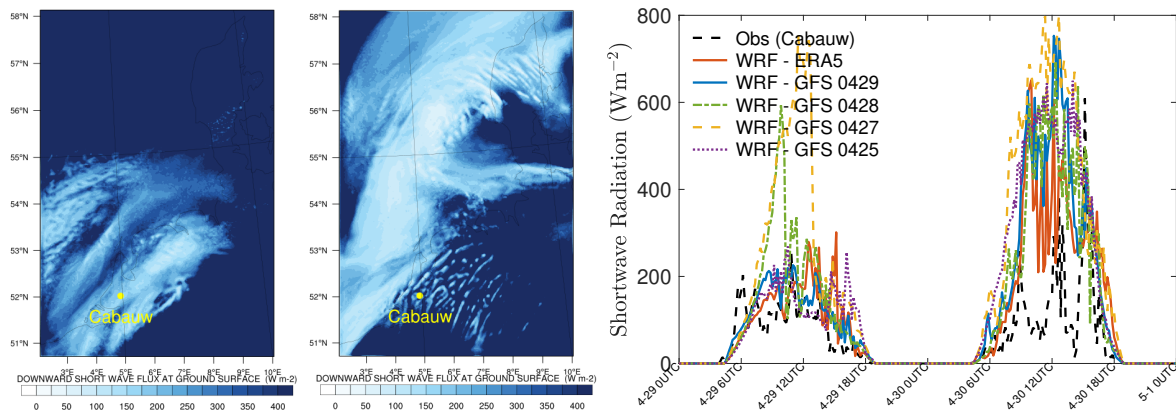


Figure 6. The WRF-ERA5-based (downwelling) shortwave radiation fields at 12 UTC on April 29th (left panel) and 30th (middle panel). Observed and simulated time-series of (downwelling) shortwave radiation at the Cabauw station are shown in the right panel.

5.4. Vertical Profiles

The time-height plots of wind speeds from the TARA radar and the WRF runs are shown in Figure 7. There are some gaps in the radar data; nonetheless, we do see certain interesting structures. For example, there is a formation of low-level jet (LLJ) around 0 UTC of April 30th. We believe that this LLJ is related to the passage of the cold front. Soon after the frontal passage, the wind speeds dropped significantly and caused the Dunkelflaute event. The observed wind speeds across the boundary layer become quite strong around 0 UTC of May 1st. All these features are well captured by the WRF-ERA5 run.

The WRF-GFS0429 and WRF-GFS0428 runs capture the evolution of the frontal LLJ and genesis of the Dunkelflaute event quite well. However, they do not show any sign of strong winds around 0 UTC of May 1st. In these respects, the performance of the WRF-GFS0427 and WRF-GFS0425 are less than satisfactory.

Observed and simulated wind profiles from Norderney and EDZE Essen locations are shown in Figure 8. The signature of frontal LLJs is clear at both the locations. In terms of capturing the heights and magnitudes of the LLJs, the performance of the WRF runs is reasonable at Norderney station. In contrast, at EDZE Essen, the WRF runs have created significantly shallower LLJs at 0 UTC. The shapes of the simulated wind profiles are significantly different from their observed counterpart at 12 UTC.

The root-mean-square error (RMSE) of wind speed profiles between the simulated and measured data in Norderney and EDZE Essen (Figure 8) are listed in the Table 1. The simulated data is interpolated to the measured heights (lower than 5 km) for 0 and 12 UTC of 30th April. From RMSE table, similar conclusions can be drawn that the performance of WRF runs in Norderney location is relatively better than at EDZE Essen. It turns out that at Norderney station, the shallower LLJs at 0 UTC and smoother wind profiles at 12 UTC of 30th April result in larger RMSE of wind speed.

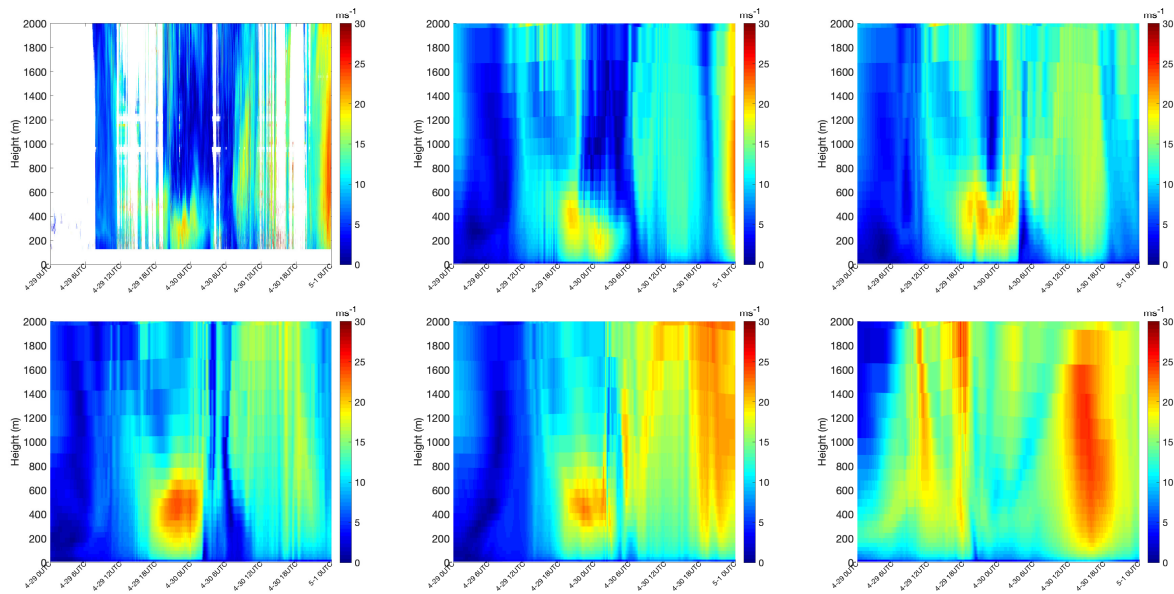


Figure 7. Time-height plots of observed (top-left panel) and simulated wind speeds below 2 km at the Cabauw observatory location. The results corresponding to WRF-ERA5, WRF-GFS0429, WRF-GFS0428, WRF-GFS0427, and WRF-GFS0425 are included in the top-middle, top-right, bottom-left, bottom-middle, and bottom-right panels, respectively.

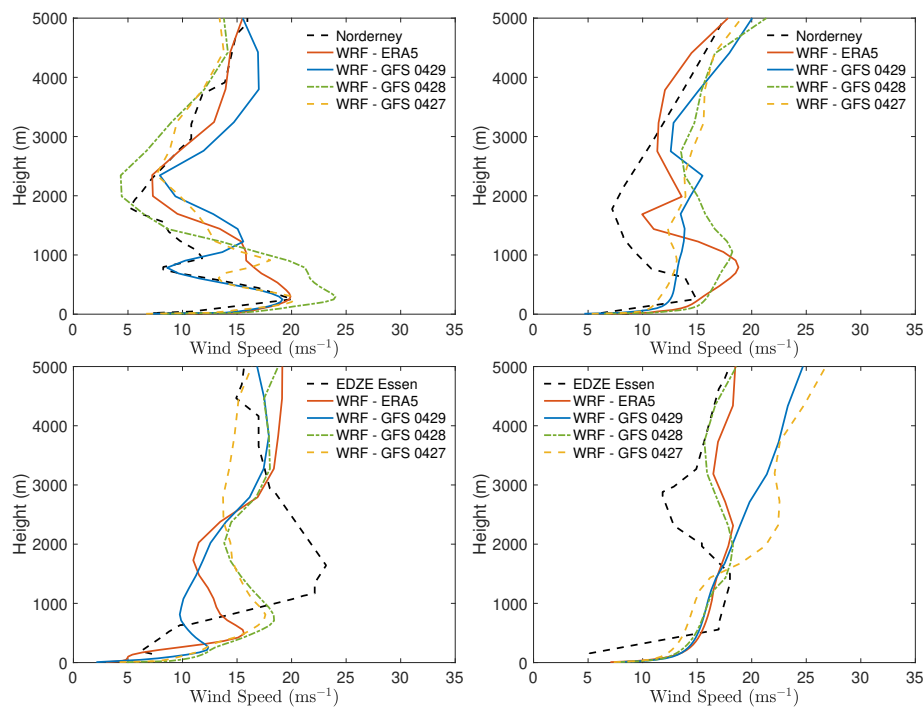


Figure 8. Observed and simulated wind speed profiles from the radiosonde launch locations named Norderney (top panel) and EDZE Essen (bottom panel). The left and right panels correspond to 0 UTC and 12 UTC of 30th April, respectively.

Table 1. RMSE (m/s) of Wind Speed Profiles

Location - UTC	WRF-ERA5	WRF-GFS 0429	WRF-GFS 0428	WRF-GFS 0427
Norderney - 0	4.15	3.32	5.87	3.96
Norderney - 12	4.73	3.84	5.97	3.51
EDZE Essen - 0	6.03	6.15	5.23	5.10
EDZE Essen - 12	3.83	5.83	3.60	7.20

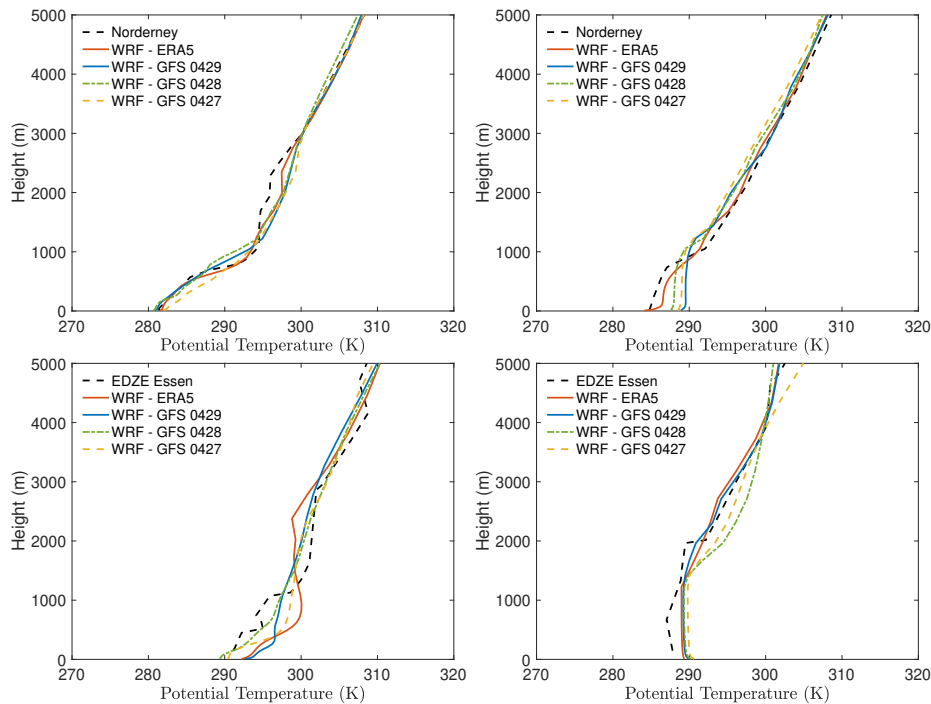


Figure 9. Observed and simulated potential temperature profiles from the radiosonde launch locations named Norderney (top panel) and EDZE Essen (bottom panel). The left and right panels correspond to 0 UTC and 12 UTC of 30th April, respectively.

In terms of the potential temperature profiles, all the WRF runs do commendable jobs. For example, they capture the stably stratified conditions at 0 UTC of April 30th. Also, at EDZE Essen, they accurately simulate the mixed layer height on 12 UTC of April 30th. However, for exactly the same time instant, they exhibit warm bias and deeper mixed layer at Norderney.

6. Conclusions

With fast-growing development of wind and solar energy generation capacity, the simultaneous deficiency of wind and solar production during a Dunkelflaute event is likely to cause increasing challenges for network operators. In this paper, taking the Dunkelflaute case in the Netherlands on 30th April 2018 as an example, an evaluation of the ability of the WRF model to forecast the event is carried out.

When compared against various observational datasets (including floating lidar, radar, met-mast, and radiosondes), it is evident that the WRF model can simulate the wind speed variations of a Dunkelflaute event reasonably well when initialized with the ERA5 reanalysis data. More importantly, by utilizing the operational GFS model-based forecasts as initial and boundary

conditions, the WRF model can also forecast such wind speed variations (albeit with slightly lesser accuracy) as long as it is initialized less than three days ahead. In contrast, the overcast condition is forecast rather poorly irrespective of the forcing dataset. The measured and simulated vertical profiles of wind speed confirmed the presence of a low-level jet during the passage of a cold front. Its relationship to the Dunkelflaute event needs to be further explored.

In the future, we would like to generalize our conclusions based on further case studies. Additionally, we would like to better understand the conditions that can lead to Dunkelflaute-type events.

Appendix A: Climatology of Dunkelflaute Events in Netherlands

We have analyzed wind and solar power production data for the years 2015–2018 (from: <https://open-power-system-data.org/>). These data have a sampling rate of 15 min; thus, in a given year, we have approximately 35,000 samples. A particular sample is classified as a Dunkelflaute event if the production by onshore wind, offshore wind, as well as, solar farms fall below 10% of their respective nominal capacities during that particular 15 min period. We do not tag a sample as a Dunkelflaute event if solar power production is exactly zero and it happens outside the time-window of 09 UTC – 15 UTC; this way, we effectively exclude nighttime conditions from the climatological analysis. It is clear from Fig. 10 that every year all the three renewable power generation systems drop below 10% of their capacities for a substantial period of time (approximately ranging from 30% to 50%). Typically, offshore wind power production has lesser downtime in comparison to their onshore counterpart. In aggregate, the Dunkelflaute events occupy around 7% – 8% of the time per year. These numbers do not vary much across the years.

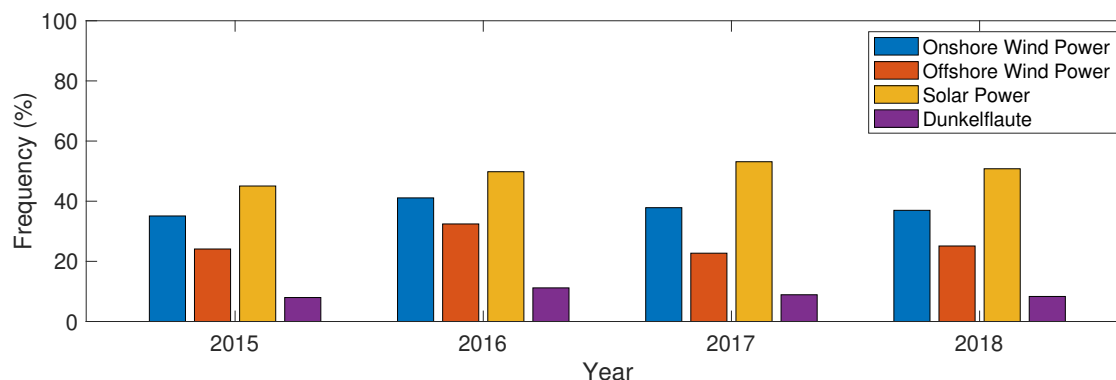


Figure 10. Percentage of the time onshore wind, offshore wind, solar power output and all three simultaneously (classified as Dunkelflaute) are less than 10% of rated output.

References

- [1] Matthias B, Andreas G and Patrick G 2019 European Energy Transition 2030: The Big Picture. Ten Priorities for the next European Commission to meet the EU's 2030 targets and accelerate towards 2050 Tech. Rep. Technical Report Agora Energiewende https://www.agora-energiewende.de/fileadmin2/Projekte/2019/EU_Big_Picture/153_EU-Big-Pic_WEB.pdf.
- [2] 2017 Energy Agenda: Towards a low-carbon energy supply Tech. Rep. Technical Report Ministry of Economic Affairs, The Netherlands <https://www.government.nl/binaries/government/documents/reports/2017/03/01/energy-agenda-towards-a-low-carbon-energy-supply/Energy+agenda.pdf>.
- [3] Huneke F, Perez Linkenheil C and Niggemeier M 2017 Cold Dunkelflaute: Robustness of the Electricity System in Extreme Weather Tech. Rep. Technical Report Energy Brain Pool, Greenpeace Energy, Berlin

- [4] NOS 2018 Network operator had to purchase large quantities of electricity to compensate for power shortage <https://nos.nl/artikel/2229787-netbeheerder-moest-groot-inkopen-om-stroomtekort-op-te-vangen.html>.
- [5] NRC 2018 Netbeheerder Tennet wendt landelijk stroomtekort af <https://www.nrc.nl/nieuws/2018/04/30/landelijk-stroomtekort-afgewend-door-netbeheerder-tennet-a1601355>.
- [6] VRT 2017 Belgium had nine-days Dunkelflaute in January https://www.vrt.be/vrtnws/nl/2017/02/24/belgie_telde_negendagendunkelflauteinjanuari-1-2900900/.
- [7] Elia 2017 Electricity Scenarios for Belgium towards 2050, Elia's Quantified Study on the Energy Transition in 2030 and 2040 Tech. Rep. Technical Report Elia
- [8] Wetzel D 2017 The Dunkelflaute brings Germany's power supply to its limit <https://www.welt.de/wirtschaft/article161831272/Die-Dunkelflaute-bringt-Deutschlands-Stromversorgung-ans-Limit.html>.
- [9] Schultz S 2017 Ist der Winter wirklich zu düster für den Ökostrom? <https://www.spiegel.de/wirtschaft/soziales/oekostrom-knapp-panikmache-mit-der-dunkelflaute-a-1133450.html>.
- [10] Fugro Norway AS 2017 Supply of Meteorological and Oceanographic data at Hollandse Kust (zuid), Monthly Progress Report Period: January 2017 Tech. Rep. Technical Report The Netherlands Enterprise Agency (RVO) <https://offshorewind.rvo.nl/windwaterzh>.
- [11] Fugro Norway AS 2017 Hollandse Kust (zuid) Field Measurement Campaign, Validation Report - January 2017 Tech. Rep. Technical Report The Netherlands Enterprise Agency (RVO) <https://offshorewind.rvo.nl/windwaterzh>.
- [12] Monna W and Van der Vliet J 1987 *Facilities for research and weather observations on the 213 m tower at Cabauw and at remote locations* (KNMI De Bilt, The Netherlands)
- [13] Verkaik J and Holtslag A 2007 *Boundary-layer meteorology* **122** 701–719
- [14] University of Wyoming 2019 Wyoming atmospheric soundings <http://weather.uwyo.edu/upperair/sounding.html>.
- [15] NCEP G 0.25 degree global forecast grids historical archive
- [16] Copernicus Climate Change Service (C3S) 2017 Era5: Fifth generation of ecmwf atmospheric reanalyses of the global climate <https://cds.climate.copernicus.eu/cdsapp#!/home>.